

Title No. 113-S06

Measured Load Capacity of Buried Reinforced Concrete Pipes

by Katrina MacDougall, Neil A. Hoult, and Ian D. Moore

Reinforced concrete pipes in North America are often designed using the Indirect Design Method, which uses bedding factors to relate in-place pipe performance to the performance obtained from three-edge bearing tests. The key performance indicator is the load at which the 0.254 mm (0.01 in.) critical crack is developed. The current bedding factors were developed using numerical modeling, and a limited amount of experimental verification has been performed to determine the accuracy of the approach. As such, a series of shallow burial tests with surface loading, a simulated deep burial test, and three-edge bearing tests were undertaken on 0.6 and 1.2 m (24 and 48 in.) diameter pipes to evaluate the current bedding factors. Both the shallow and deep burial tests indicated that the critical crack does not develop until after the specified service load has been surpassed, suggesting that current pipe designs are overly conservative.

Keywords: buried pipe; crack widths; Indirect Design Method; reinforced concrete.

INTRODUCTION

The AASHTO (2013) LRFD Bridge Design Code specifies two methods for the design of reinforced concrete pipe: Indirect Design and Direct Design. The Indirect Design Method attempts to relate the critical load obtained during three-edge bearing tests conducted by the pipe manufacturer (ASTM C497-13) to the capacity of the pipes in-place through a modification factor known as the bedding factor. The critical load is specified as the load at which a 0.254 mm (0.01 in.) crack forms inside the pipe. However, there has been limited experimental testing undertaken to determine whether the bedding factors are appropriate, as they are based on the results of numerical analysis (McGrath 1993).

To address this knowledge gap in reinforced concrete pipe design, a research program was undertaken with the following objectives: 1) to measure the diameter changes, strains, and crack widths that develop in the pipe wall for shallow burial under surface loads and under simulated deep burial loading; 2) to conduct ultimate limit state tests on the buried pipes to determine the load at which the critical crack width develops; 3) to obtain three-edge bearing test data to support the Indirect Design calculations; and 4) to compare these results to Indirect Design estimates.

The paper outlines previous research, the experimental program, the pipe specimens, the instrumentation, and the test setup for the full-scale tests on the buried reinforced concrete pipe specimens. The results of the testing program are then presented and discussed.

RESEARCH SIGNIFICANCE

Reinforced concrete pipes are often designed using the Indirect Design Method, which employs bedding factors to correlate the performance of pipes tested in three-edge

bearing to their performance in place. A limited amount of testing has been conducted on buried pipes to evaluate whether these bedding factors are appropriate. To address this knowledge gap, a series of buried reinforced concrete pipe experiments was undertaken at both shallow burial under surface loading and simulated deep burial to evaluate the pipe performance. These results were then combined with three-edge bearing test results to evaluate the appropriateness of the bedding factors.

BACKGROUND

There has been limited full-scale buried pipe testing performed to assess the effect of surface loading on reinforced concrete pipes. Testing performed by Wong et al. (2006) used pressure sensors installed on small-diameter (less than 0.9 m [36 in.]) reinforced concrete pipes buried in the field in areas under high traffic loading. When the pressure sensor results were compared to the Indirect Design estimates, it was found that the equations resulted in overly conservative soil stresses.

Becerril García and Moore (2013) (also refer to Moore et al. [2012]) performed surface load tests on buried 0.6 and 1.2 m (24 and 48 in.) diameter pipes. Although the work focused on the structural response of pipe joints, the particular test pipes were consistently found to be able to carry service loads without cracking, which is the critical limit state of the Indirect Design Method.

Field tests were performed by Erdogmus and Tadros (2009) on 1.2 m (48 in.) diameter pipe with a wall thickness of 127 mm (5 in.) under varying depths of embankment earth loading. Additionally, these same pipes were tested in three-edge bearing. In the buried test, strain gauges on the reinforcement cage at the crown, invert, springline, haunch, and shoulder (the critical locations around the pipe circumference are illustrated in Fig. 1) were used to monitor the development of strain in the reinforcement under earth loads. Erdogmus and Tadros found the test pipe resisted a 50-D (Class II-equivalent) D-Load in the three-edge bearing test, which corresponds to a maximum cover depth of 3 m (10 ft). However, under buried conditions the pipe steel reinforcement had not even reached yielding at 6 m (20 ft) of cover. These results show that the relationship between three-edge bearing performance and buried conditions may not be accurately captured by the current bedding factors;

ACI Structural Journal, V. 113, No. 1, January-February 2016.

MS No. S-2014-296.R1, doi: 10.14359/51688059, received April 15, 2015, and reviewed under Institute publication policies. Copyright © 2016, American Concrete Institute. All rights reserved, including the making of copies unless permission is obtained from the copyright proprietors. Pertinent discussion including author's closure, if any, will be published ten months from this journal's date if the discussion is received within four months of the paper's print publication.

Table 1—Test program overview

Test program	Facility	Diameter, m	Diameter, in.	Loading type	Depths, ft	Depth, m
A	West test pit	0.6	24	Earth and simulated vehicle	1, 2, and 4	0.3, 0.6, and 1.2
A	West test pit	1.2	48	Earth and simulated vehicle	1, 2, and 4	0.3, 0.6, and 1.2
B	Biaxial cell	0.6	24	Earth load (deep burial)	1 to 152*	0.3 to 46.3*
C	Load frame	1.2	48	Three-edge bearing	Unburied	Unburied

*Equivalent depth of burial for soil of density of 20.42 kN/m³ (130 lb/ft³).

Table 2—Pipe specimen properties

Pipe inner diameter, mm	Wall type	Wall thickness, mm (in.)	Class equivalent	f'_c , MPa (ksi)	f_y , MPa (ksi)	f_{ut} , MPa (ksi)	Wire gauge, mm ² (in. ²)	Spacing, mm (in.)	Area of steel, mm ² /m (in. ² /ft)	
									Inside	Outside
600	C	94 (3.75)	IV	70.0 (10.1)	595 (86.3)	625 (90.6)	16.1 (0.025)	76 (3.0)	212 (0.100)	NA
600	C	94 (3.75)	V	66.0 (9.6)	585 (84.8)	597 (86.6)	25.8 (0.04)	68 (2.7)	380 (0.179)	NA
1200	B	125 (5)	III	57.6 (8.4)	485 (70.3)	550 (79.8)	25.8 (0.04)	51 (2.0)	506 (0.239)	506 (0.239)
1200	C	144 (5.75)	III	57.6 (8.4)	485 (70.3)	550 (79.8)	25.8 (0.04)	68 (2.7)	380 (0.179)	380 (0.179)

Note: NA is not available.

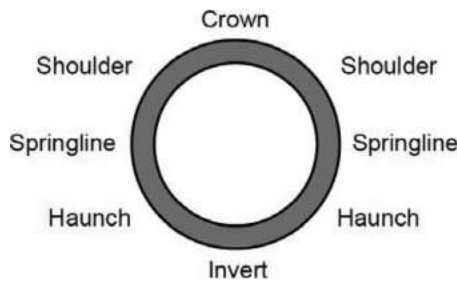


Fig. 1—Critical regions around pipe circumference.

however more experimental evidence with different pipes and burial conditions is required.

Lay and Brachman (2014) performed tests on 0.6 m (24 in.) diameter pipes under 0.3, 0.6, and 0.9 m (1, 2, and 3 ft) cover depths. Under fully factored CL-625 (the Canadian design truck – CSA [2006]) single-axle loading of 400 kN (90 kip) at 0.3 m (1 ft) of cover, and using the measured strain, the circumferential bending moment in the pipe wall was calculated and found to be lower than predicted by the code (CSA 2006).

The previous research indicates that there is a need for further testing of reinforced concrete pipes to evaluate the Indirect Design Method, which is detailed in the following sections.

EXPERIMENTAL INVESTIGATION

The experimental campaign consisted of three test programs. Program A involved shallow burial experiments with surface loading using both 0.6 m (24 in.) and 1.2 m (48 in.) diameter pipes. Program B investigated the effects of deep burial on a 0.6 m (24 in.) diameter pipe. Program C involved performing three-edge bearing tests on 1.2 m (48 in.) diameter pipes to be used in conjunction with three-edge bearing test results for the 0.6 m (24 in.) pipes obtained from previous investigations. The test programs and specimens are summarized in Table 1.

Specimens

For Program A, two 0.6 m (24 in.) diameter pipes were tested: a Class IV-equivalent pipe with wall type C (Wall C)

and a Class V-equivalent pipe with Wall C. All the pipes used in the testing program were manufactured in accordance with ASTM C655M-14, so references to pipe strength classes throughout this research represent equivalent classes. This means the pipes do not have the steel reinforcement specified in ASTM C76-11, but instead achieve the same minimum D-load capacity as the equivalent ASTM C76 pipe would. Both the Class IV and Class V-equivalent pipes had a wall thickness of 94 mm (3.75 in.) and a length of 2.44 m (8 ft), including the bell but excluding the spigot. Two 1.2 m (48 in.) diameter pipes were also tested in Program A: a Class III-equivalent pipe with Wall B, and a Class III-equivalent pipe with Wall C. The Wall B pipe had a wall thickness of 125 mm (5 in.) and the Wall C pipe had a wall thickness of 144 mm (5.75 in.). Both pipes had an internal diameter of 1.2 m (48 in.) with a length of 2.44 m (8 ft), including the bell but excluding the spigot. A summary of all test pipe specimen dimensions and material properties is given in Table 2. For Program B, a 0.6 m (24 in.) Class IV-equivalent Wall C pipe with the same properties as the Class IV pipe in Program A was used. For Program C, the three-edge bearing data was provided by previous testing for the 0.6 m (24 in.) pipes. According to manufacturer’s data, the 0.6 m (24 in.) Class IV-equivalent pipe used for Test Programs A and B reached a cracking D-Load of 144 N/m/mm (3000 lbf/ft/ft) with a crack width of 0.30 mm (0.012 in.) and reached an ultimate failure D-load of 159 N/m/mm (3326 lbf/ft/ft). The D-Load for the 0.6 m (24 in.) Class V-equivalent pipe was approximately 149 N/m/mm (3125 lbf/ft/ft), based on data reported by Becerril Garcia (2012), who performed three-edge bearing tests on other samples from the same batch of pipes. Both pipes exceeded the cracking performance specifications for a Class V pipe. Three-edge bearing tests were conducted on the 1.2 m (48 in.) Class III-equivalent Wall B and Wall C pipes in Program C.

Program A

The following section outlines the shallow burial experiments that were undertaken in the 7.6 x 7.6 x 3 m (25 x 25 x 9.8 ft) deep test pit (Moore 2012) at the GeoEngineering lab at Queen’s University.

Instrumentation: Program A—Before burial, each of the pipes was instrumented with eight strain gauges oriented to measure strain in the circumferential direction of the pipe, four around the outside circumference and four around the inside circumference of the pipe at the crown, invert, and springlines (refer to Fig. 1 for crown, invert, and springline locations). To ensure that the strains being measured represented average strains rather than localized strains across an individual piece of aggregate, the size of the strain gauge was specifically chosen to be at least three times larger than the largest aggregate size. The gauges used were 51 mm (2 in.) in length with a resistance of $120\ \Omega$ ($\pm 0.2\%$) and gauge factors of 1.100 and 1.110. The strain gauges were located directly beneath the steel loading pad that was connected to the hydraulic actuator and was used to provide the same footprint as an AASHTO (2013) wheel pair (refer to Fig. 2).

Four displacement transducers were installed in each pipe segment to measure changes in horizontal and vertical diameter at two locations in the pipe. The displacement transducers were installed so that both sets of displacement transducers were the same distance from the end of the pipe on either side of the wheel pad loading location (refer to Fig. 2).

Two cameras were mounted in each pipe to monitor longitudinal crack development at the crown and invert. The cameras were mounted near the wheel pad loading point. Digital images were taken throughout the test at approximately 50 kN (11.24 kip) increments. The images were processed using an image analysis technique known as particle image velocimetry (PIV) or digital image correlation (DIC) (refer to Take [2015]) to measure the crack widths. DIC enables areas of interest, known as patches, to be tracked by comparing images taken while the pipe is under load to an initial image taken before loading, known as the reference image. If two patches on either side of the crack are tracked throughout the loading process, then the crack width can be determined. A DIC software package specifically for geotechnical applications was used to measure the displacements of the patches (White et al. 2003).

The use of DIC to measure crack widths is advantageous, as *a priori* knowledge of the crack locations is not required and an average crack width along the length of the crack can be determined. A number of researchers have used DIC to measure crack widths in concrete and have verified the accuracy of this technique (Küntz et al. 2006; Destrebecq et al. 2011). There is also a newer variation of DIC that uses two cameras to measure three-dimensional (3-D) displacements, known as 3-D DIC, but the majority of research and evaluation work for the measurement of cracks in reinforced concrete has been undertaken with two-dimensional (2-D) DIC, so this technique was employed herein. Dutton et al. (2014) undertook a series of experiments comparing the strains calculated from displacement measurements from GeoPIV to strains measured using conventional strain gauges on steel beams, and showed that the GeoPIV values had similar accuracy.

However, one of the challenges of using DIC to measure the crack widths is that, as the pipe displaces under load, it moves closer to the camera, which can cause measurement errors due to this out-of-plane movement (Hoult et al.

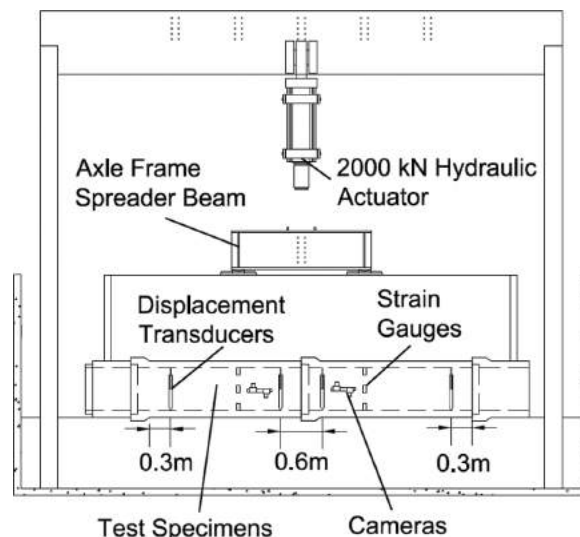


Fig. 2—Elevation view of 0.6 m (24 in.) pipe test configuration showing strain gauge and displacement transducer locations (1.2 m [48 in.] pipe testing configuration similar). (Note: 1 m = 39.37 in.; 1 kN = 224.8 lbf.)

2013). Hoult et al. showed that out-of-plane effects can be mitigated by using known measurements in the field of view, and they demonstrated the technique by comparing the DIC measurements to strain rosette measurements on steel plates. Additionally, when measuring the displacement between two patches across the crack, this displacement is due to the combined effects of the crack opening and the tensile strain that is developed in the pipe between the two patches.

To overcome these challenges, the techniques suggested by Hoult et al. (2013) were employed by measuring the displacement between four patches placed on either side of the crack, as illustrated in Fig. 3(a). Patch numbers 2 and 3 were used to measure uncorrected crack widths taken as the change in distance X_2 . The measured lengths X_1 and X_3 were averaged together for each load stage. Because the crack did not form between the two outer rows of patches, any changes in the lengths X_1 and X_3 during the test would be due to effects of out-of-plane movement and tensile strains. Thus, the X_2 displacement values were adjusted by subtracting the average of X_1 and X_3 from X_2 to determine the change in length due to crack opening. Sixteen rows of four patches were used to measure each crack and the average crack width was employed. Example patch layouts are shown in Fig. 3(b). Finally, a scale was fixed to the pipe in the field of view of the cameras to determine a pixel-to-length ratio for the DIC analysis, as DIC measures displacement in pixels, but also so that the 0.25 mm (0.01 in.) crack width could be confirmed visually (refer to Fig. 3(b)). When the cracks reached a sufficient width, it was possible to compare the crack widths measured using DIC to the scale included in the image (Fig. 3(b)), and the measurements showed good agreement.

Burial Conditions: Program A—Test Program A was conducted using an embankment installation. To prevent interaction with the rigid boundary condition created by the concrete floor of the test pit, soil bedding that was 900 mm (35 in.) deep was prepared, with an additional 100 mm (4 in.) of loose bedding to help prevent voids at the haunches for

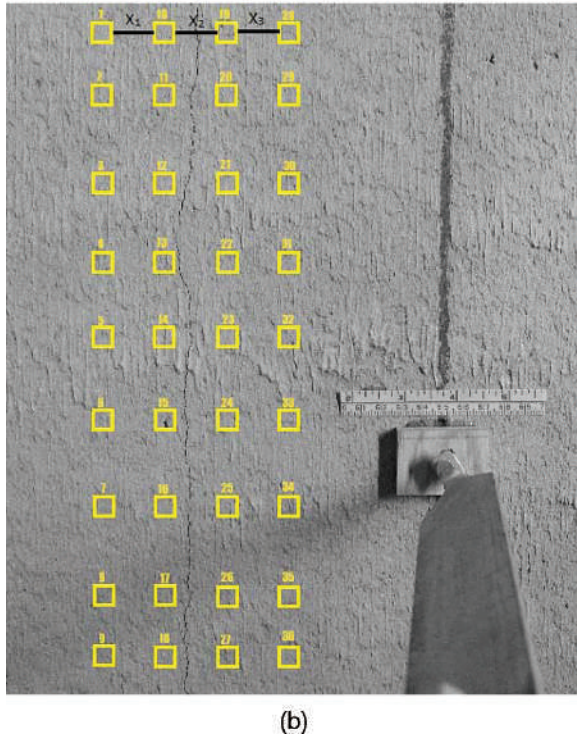
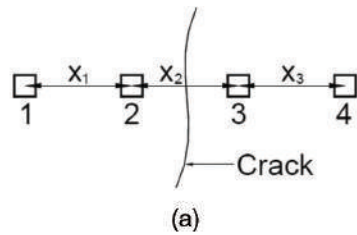


Fig. 4—0.6 m (24 in.) diameter pipes before burial with Class IV pipe on the right and Class V pipe on the left.

(GP-SP) in accordance with Type 2 burial conditions as per AASHTO (2013) to a minimum of 90% standard Proctor.

Loading regime: Program A—The pipes in test Program A were tested in eight stages involving cover depths of 1.2, 0.6, and 0.3 m (4, 2, and 1 ft). The service load testing on the pipe was performed using a pair of steel plates to simulate the single axle of the AASHTO design truck applied at the ground surface above the buried pipes. Using a steel axle frame spreader beam with steel pads to represent wheel pairs at each end of the axle, the test pipes were loaded simultaneously by a 2000 kN (450 kip) hydraulic actuator, as can be seen in Fig. 2 and 5. The steel wheel pads were 254 x 508 mm (10 x 20 in.), as specified by AASHTO (2013), and were loaded by the steel axle frame with the wheel pads separated by 1.8 m (6 ft). The axle frame was aligned over the longitudinal axis of the pipe to simulate a truck travelling perpendicular across the pipe's longitudinal axis (the most common alignment for culvert pipes crossing under roadways, and the one that places both ends of the axle over the pipe). At each load stage and cover depth (1.2, 0.6, and 0.3 m [4, 2, and 1 ft]), the loads were cycled between zero and the maximum load for that load stage three times to ensure the soil beneath the load pads was compacted and that the results were obtained for first loading, where permanent as well as recoverable deformations can be expected, and for the second and third load cycles where recoverable, elastic deformations dominated.

To limit bearing failure of the soil under the loading pads during the ultimate limit states tests, enlarged wooden bearing pads 950 mm (37.5 in.) long and 370 mm (14.6 in.) wide were placed below the steel pads. Additionally, the load was applied to each pipe individually rather than to both pipes simultaneously through a spreader beam, as was the case for the service load tests (that is, each pipe was loaded to its ultimate limit state using a single loading plate representing a wheel pair). At the burial depth used for this test—0.3 m (1 ft)—the interactions between the wheel pairs at each end of the pipeline are modest, so the effect of the second wheel pair would also likely have been modest.

According to the AASHTO LRFD (AASHTO 2013) loading conditions, pipes buried at 0.3 m (1 ft) should be able to resist a live wheel load of 71 kN (16 kip), factored

Fig. 3—Layout of patches for crack measurements using DIC: (a) outer measurements X_1 and X_3 are used to correct crack width measurement X_2 for strain and out-of-plane movement; and (b) patch locations shown on image of cracked concrete pipe showing scale used to convert pixel measurements to measurements in mm (in.).

the 0.6 m (24 in.) pipes. The pipes were then buried in 150 to 300 mm (6 to 12 in.) lifts to a maximum cover depth of 1.2 m (4 ft). The soil was compacted using both small and large vibrating plate compactors to achieve the required soil conditions after the addition of every soil lift. A nuclear densometer was used to gather density, percent water content, and percent standard Proctor maximum dry density (SPMDD) readings within each lift to ensure that the entire burial was consistent and achieved minimum required soil density. The 0.6 m (24 in.) pipes can be seen prior to burial in Fig. 4, with the Class IV-equivalent pipe on the right side of the image and the Class V-equivalent pipe on the left side. The burial process for the 1.2 m (48 in.) pipes was similar to that used for the smaller-diameter specimens except that a compacted soil foundation of 635 mm (25 in.) was prepared on top of the rigid concrete floor with an additional 76 mm (3 in.) of loose bedding.

A self-leveling laser level was used to ensure that lifts were consistent and did not exceed 300 mm (12 in.). The pipes in test Program A were installed in poorly graded sandy gravel

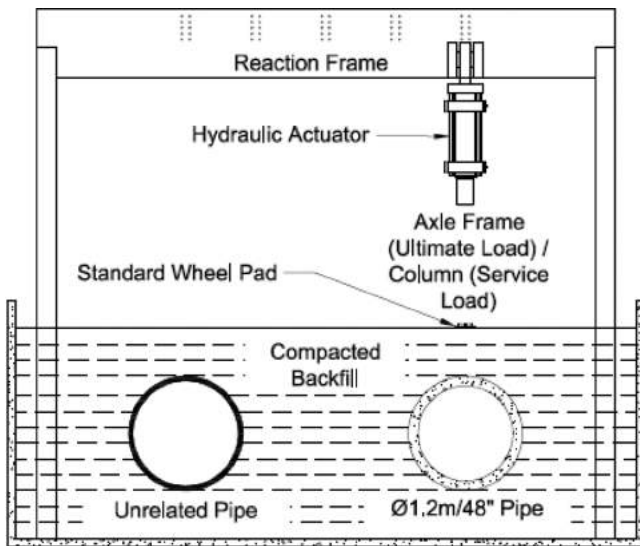


Fig. 5—Shallow burial (Program A) testing configuration for 1.2 m (48 in.) diameter pipe (0.6 m [24 in.] diameter pipe testing configuration similar).

by a dynamic load allowance of 1.289 and a multi-presence factor of 1.2, resulting in a service load of 110 kN (25 kip). After further multiplication by the live load factor of 1.75, an ultimate load of 193 kN (43 kip) results.

Test Program B

The following section outlines the testing performed on a 0.6 m (24 in.) diameter pipe under simulated deep burial in the biaxial test cell at the GeoEngineering lab at Queen's University.

Instrumentation: Program B—The 0.6 m (24 in.) diameter pipe was outfitted with eight strain gauges oriented in the circumferential direction, four around the outside circumference and four around the inside circumference of the pipe at the crown, invert, and springlines. The strain gauges were located around the central transverse cross section of the pipe. The displacement transducers were installed so that both sets of displacement transducers were the same distance from the end of the pipe. Two DSLR cameras were installed to monitor crack development at the crown and invert as discussed for Program A.

Burial conditions: Program B—The biaxial test cell is a 2 x 2 x 1.6 m (6.5 x 6.5 x 5.2 ft) deep steel box with a rubber bladder under the lid that can be pressurized with air and used to apply a uniform pressure on the ground surface to simulate deep burial. The pipe was horizontally centered in the cell, as can be seen in Fig. 6, with 0.6 m (24 in.) between the wall of the pipe specimen and the edge of the cell on each side, and 0.2 m (8 in.) of soil under the pipe invert. A double-layered friction treatment was applied to each wall of the cell to reduce the effects of friction between the soil and the cell wall. First, a single layer of polyethylene sheeting was attached to the four vertical walls of the biaxial cell and then lubricated with specially selected silicon grease. A second sheet of polyethylene was then used to cover the first lubricated sheet without securing it to the cell walls in any other way. The friction treatment within the biaxial cell is described in greater detail by Tognon et al. (1999).

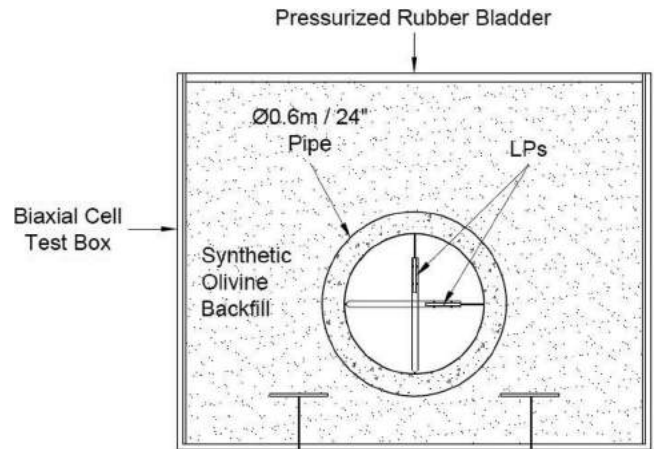


Fig. 6—Simulated deep burial (Program B) testing configuration showing pipe inside pressure cell.

The pipe in Program B was buried in synthetic olivine sand in lifts of 0.3 m (12 in.). Once again, a nuclear densometer was used to gather density, percent water content, and percent standard Proctor maximum dry density (SPMDD) readings within each lift to ensure that the entire burial was consistent and achieved minimum required SPMDD. The soil had an average dry density of 15.87 kN/m³ (101 lb/ft³), a water content of 0.5%, and a SPMDD of 71%.

Loading Regime: Program B—The pressure in the bladder and, thus, the vertical pressure in the cell, was steadily increased at a rate of approximately 35.2 kPa/min (5.1 psi/min), which was equivalent to 2.2 m (7.3 ft) of soil cover/min. The test was run to a maximum pressure of 700 kPa (102 psi), approximately equal to a burial depth of 44 m (145 ft) using the density of synthetic olivine backfill, or 34 m (113 ft) of material with a typical embankment design density of 20.42 kN/m³ (130 lb/ft³).

Test Program C

These tests were conducted on the 1.2 m (48 in.) diameter pipe using the standard three-edge bearing setup as outlined in ASTM C655M-14. The diameter change was recorded using string potentiometers and the load was measured using a load cell; both sets of data were logged using a data acquisition system. The crack widths were monitored using the digital camera setup.

EXPERIMENTAL RESULTS AND DISCUSSION

Diameter change: Program A

For the 0.6 m (24 in.) pipes, both the Class IV and Class V-equivalent pipes experienced less than 1% vertical diameter change during the ultimate load test at 0.3 m (1 ft) burial depth, as can be seen in Fig. 7(a). The diameter changes at greater cover depths (0.6 and 1.2 m [2 and 4 ft]) were lower, indicating that, as expected, the critical pipe behavior occurs at the minimum cover depth. Up to the factored service load of 110 kN (24.7 kip), the pipe behavior is linear with very small changes in diameter. After cracking occurs at approximately 270 kN (60 kip), which is much higher than both the service load and the design ultimate load of 193 kN (43 kip), the change in diameter becomes nonlinear and the stiffness decreases, as can be seen in Fig. 7(a). Before

cracking occurs, the vertical diameter change in both pipes is almost the same. However, after cracking, the Class IV pipe experiences greater vertical diameter change than the Class V pipe. This behavior is expected because both pipes have the same wall thickness and similar concrete strengths, which controls the bending stiffness prior to cracking. However, the Class V pipe has a greater area of steel, which results in higher bending stiffness post-cracking. One can also see a variation in the change in diameter with location along the pipe with larger diameter changes occurring under the loading point. This indicates that, while there is load distribution along the length of the pipe, the critical section of the pipe for analysis is directly underneath the applied load.

For the 1.2 m (48 in.) pipes, the diameter change is also less than 1% prior to cracking during the ultimate limit state test at 0.3 m (1 ft) burial depth, as can be seen in Fig. 7(b). However, in this case, there are differences between the two pipes prior to cracking, as the Wall B pipe, which is thinner, experiences greater diameter change than the Wall C pipe. This is to be expected because the bending stiffness of the thinner wall pipe will be lower, leading to higher deflections. Similar to the 0.6 m (24 in.) pipes, the cover depth used during these buried pipe strength tests was 0.3 m (12 in.) and the critical cross section was directly underneath the applied load.

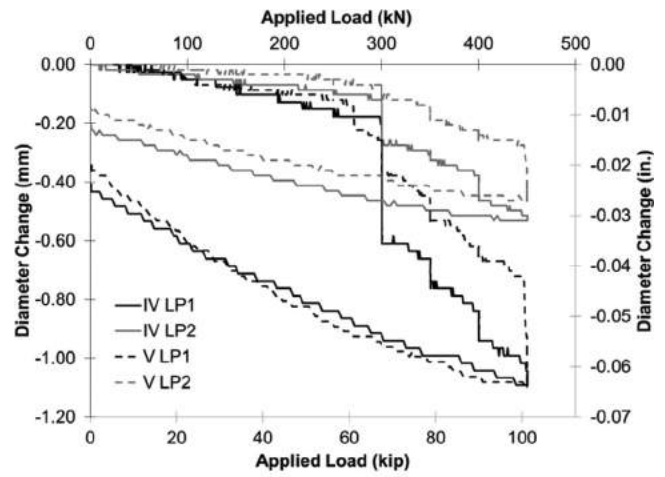
Strain behavior: Program A

The change in curvature around the circumference of the pipe wall, ϕ , was found using the inner and outer face strain readings and the wall thickness, as per Eq. (1), while the average circumferential strain, $\epsilon_{average}$, in the pipe wall was found using the strain readings and Eq. (2). Changes in curvature are subsequently called curvature, and these are not the same as the inverse of pipe radius for this cylindrical structure.

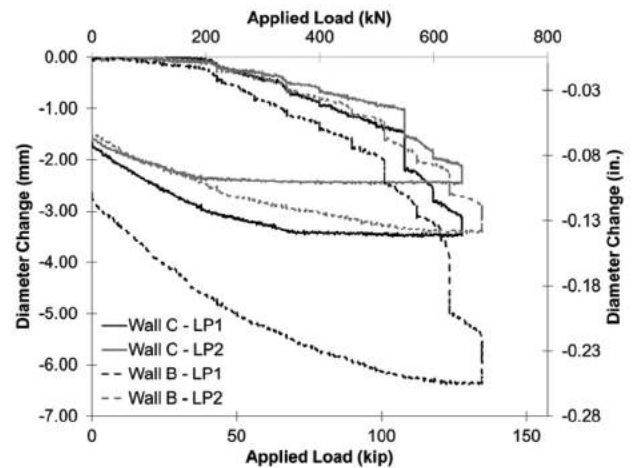
$$\phi = \frac{\epsilon_{inside} - \epsilon_{outside}}{h} \quad (1)$$

$$\epsilon_{average} = \frac{\epsilon_{inside} + \epsilon_{outside}}{2} \quad (2)$$

The strain results from the ultimate load test were used to determine the curvature in the pipe at the crown, invert, and springlines, as shown in Fig. 8(a) for the 0.6 m (24 in.) pipes and in Fig. 8(b) for the 1.2 m (48 in.) pipes. For clarity, only the results at one springline are plotted, although the behavior at the other springline is similar. The average strain results are presented in Fig. 9(a) for the 0.6 m (24 in.) pipes and in Fig. 9(b) for the 1.2 m (48 in.) pipes. The concrete surface strain gauges can only effectively measure the strain until the pipe begins to crack in the area of the strain gauge. Thus, Fig. 8 and Fig. 9 show only the strain data measured up until the point of cracking in the area of the gauges and, in some cases, until just after cracking to highlight the nonlinear behavior of the pipe after cracking (although the values of strain after cracking are potentially erroneous). The strain gauge located at the outside crown of the Class IV-equivalent



(a) 0.6 m / 24 in. diameter pipe specimens.

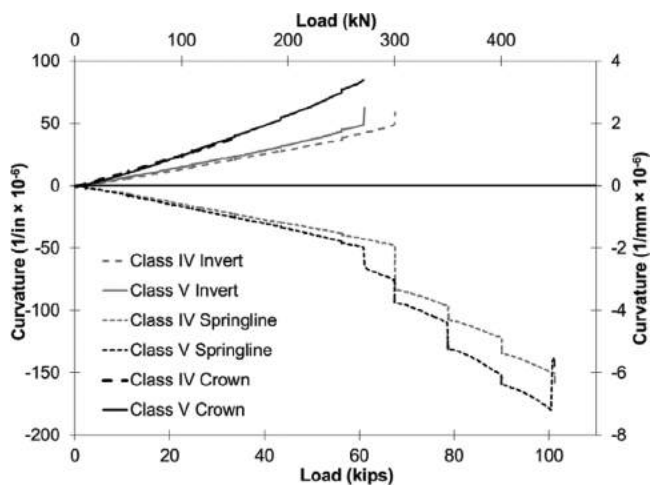


(b) 1.2 m / 48 in. diameter pipe specimens.

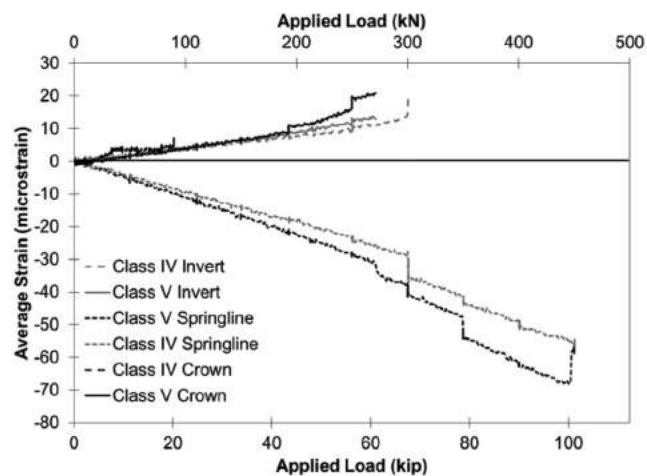
Fig. 7—Diameter change versus applied load (Program A).

pipe was damaged early in the maximum load test and, therefore, curvature in the pipe at the crown is shown only up to 151 kN (34 kip).

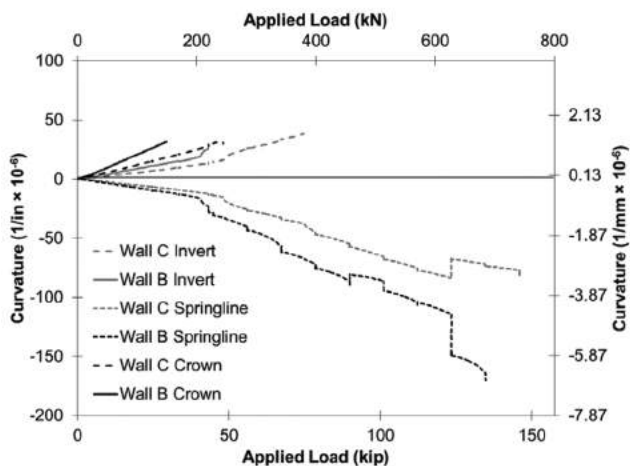
Figure 8(a) shows that curvature changes due to the applied load for both the Class IV and Class V-equivalent pipes developed almost linearly with applied load, and were nearly equal to one another before cracking occurred. This is because both pipes have the same outer diameter and so should experience the same moments in the elastic range. Both pipes also have the same wall thickness and similar concrete strengths, f'_c , with only a 6% difference, resulting in nearly identical flexural rigidity (EI values) and leading to almost the same curvatures. Additionally, the curvature changes at the crowns of both pipes are greater than those at the inverts. This is because at shallow burial depths, the crown would develop the greatest curvature due to the closer proximity to the surface load being applied. For the 1.2 m (48 in.) pipes, it can be seen from Fig. 8(b) that the curvature developed linearly until cracking occurred between approximately 133 to 222 kN (30 to 50 kip). The curvature of the Wall B pipe exceeds that of the Wall C pipe for each measurement location due to the lower flexural rigidity of the thinner pipe (Wall B) and leading to greater curvatures when the moments are the same. It is interesting to note that



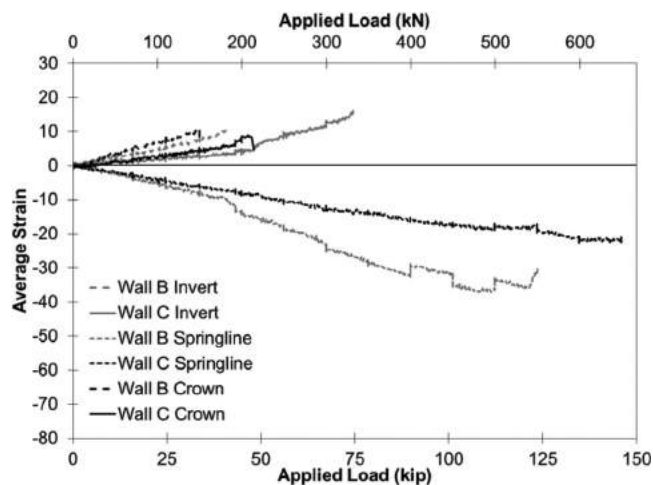
(a) 0.6 m / 24 in. diameter pipe specimens.



(a) 0.6 m / 24 in. diameter pipe specimens.



(b) 1.2 m / 48 in. diameter pipe specimens.



(b) 1.2 m / 48 in. diameter pipe specimens.

Fig. 8—Curvature versus applied load (Program A).

the strains in these pipes did not exceed the cracking strain in the concrete until after the service load (110 kN [24.7 kip]) had been reached. Because the service load is used when evaluating the fatigue capacity of the structure, this suggests that for the pipes tested here, fatigue will not be an issue as the stress range is less than the cracking stress for concrete, by an adequate factor of safety.

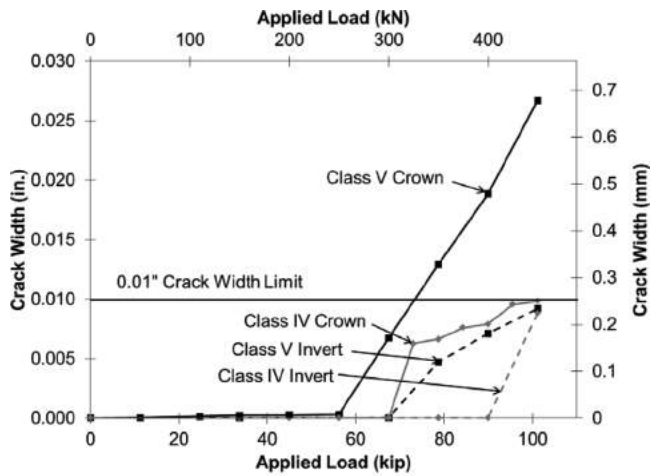
Figure 9(a) shows that the average strain for the 0.6 m (24 in.) pipes develops linearly with load and is nearly the same prior to cracking. These results are as expected; the outside diameters are identical, so the thrusts and average strains should be similar. Although the magnitude of the strains are less than 100 microstrain, due to the high axial stiffness of the pipe wall, every 10 microstrain represents an axial force in the pipe wall of approximately 35 kN/m (2.40 kip/ft). This is important to note because the moment resistance of reinforced concrete members is influenced by the amount of axial force. Figure 9(b) shows that the Wall C pipe developed, on average, only 37% of the average strain of the Wall B pipe at the crown, which is due in part to the larger cross section of the Wall C pipe developing lower axial stresses.

Fig. 9—Average strain versus applied load (Program A).

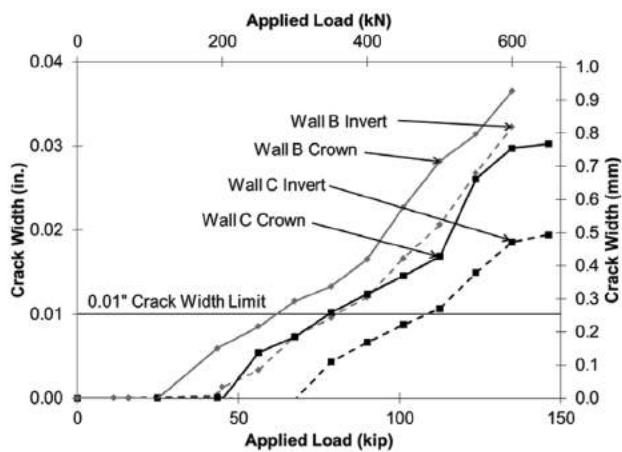
Crack widths: Program A

Figure 10(a) shows the applied load versus measured crack widths during the ultimate limit state tests on the 0.6 m (24 in.) diameter pipes. The first sign of visible cracking occurred in the Class V-equivalent pipe at the crown at an applied load of approximately 250 kN (56 kip) and was followed by cracking at the invert at approximately 298 kN (67 kip). The first sign of visible cracking in the Class IV-equivalent pipe occurred at the crown at approximately 298 kN (67 kip) and was followed by cracking at the invert at approximately 400 kN (90 kip). In both cases, cracking first occurred at the crown followed by cracking at the invert. This is thought to be due to the greater load attenuation at the invert in the shallow burial tests (loads spread out from the ground surface to a much greater extent at the depth of the invert of 0.9 m [3 ft] than at the depth of the crown of 0.3 m [1 ft]). It is worth noting that cracking occurred well after the design service load of 110 kN (25 kip) and even after the design ultimate load of 193 kN (43 kip).

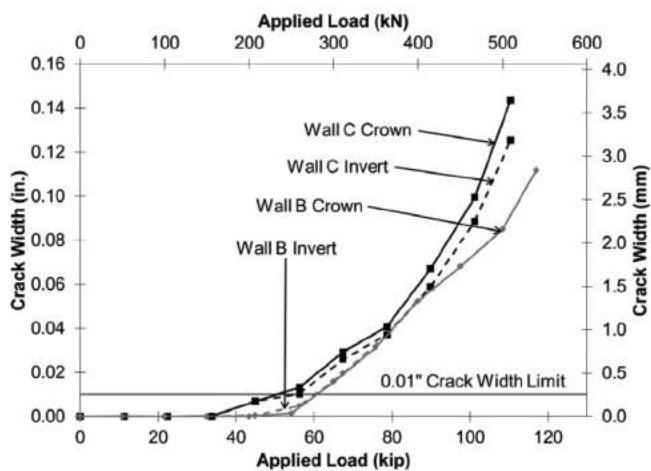
Crack widths monitored during the ultimate limit states tests on the 1.2 m (48 in.) pipes are presented in Fig. 10(b). The first sign of visible cracking occurred in the Wall B pipe at the crown at an applied load of approximately 110 kN



(a) 0.6 m / 24 in. diameter pipe specimens



(b) 1.2 m / 48 in. diameter shallow burial pipe specimens



(c) 1.2 m / 48 in. diameter three edge bearing pipe specimens

Fig. 10—Crack width versus applied load (Programs A and C). (Note: 1 in. = 25.4 mm.)

(25 kip) and was followed by cracking at the invert at an applied load of approximately 200 kN (45 kip). The first sign of visible cracking in the Wall C pipe occurred at the crown at an applied load of approximately 200 kN (45 kip) and was later followed by cracking at the invert at approximately

298 kN (67 kip). Cracking developed first in the Wall B pipe, as expected, due to the lower wall thickness. If the moments and concrete modulus are the same and the impacts of hoop force are neglected, strain to induce cracking should occur in the Wall B pipe at loads $(5/5.75)^2$ or 76% of those for the Wall C pipe. However, the ratio from the experimental results is $25/45 = 56\%$. Possible explanations for this difference include differences in the concrete moduli, small imperfections in the pipes, different initial strains resulting from earth loading and the prior loading history, or differences in soil support provided to the two different pipes. However, even the Wall B pipe did not develop the critical crack width of 0.25 mm (0.01 in.) until an applied load of 275 kN (62 kip), which once again exceeds both the design service and ultimate loads.

Diameter change: Program B

The pipe vertical diameter change versus applied pressure is given in Fig. 11(a). The pipe responded linearly to the applied pressure until approximately 280 kPa (41 psi), which is equivalent to a burial depth of 14 m (46 ft). The graph then shows two minor dips, which correspond to the development of cracks, followed by a reduction in stiffness but still approximately linear behavior. At approximately 415 kPa (60 psi) of overburden pressure, there is a significant decrease in the stiffness of the pipe coupled with a change to a nonlinear response due to increased cracking in the pipe and the start of yielding of the steel reinforcement. The pipe reached a deflection of 4.10 mm (0.16 in.) at an overburden pressure of 700 kPa (102 psi), which is equivalent to a burial depth of 34 m (113 ft) before the test was halted.

Strain behavior: Program B

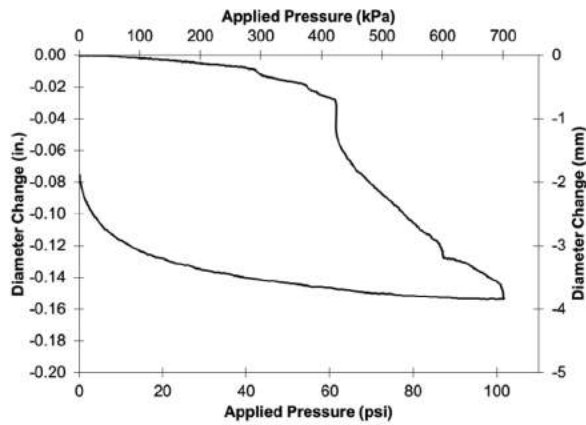
As opposed to the shallow burial test pipes, which had maximum curvature at the crown, the simulated deep burial pipe had maximum curvature at the invert as shown in Fig. 11(b). The pipe behavior in terms of both curvature and average strain was linear until cracking began at between 262 and 297 kPa (38 and 43 psi) of overburden pressure.

Crack width: Program B

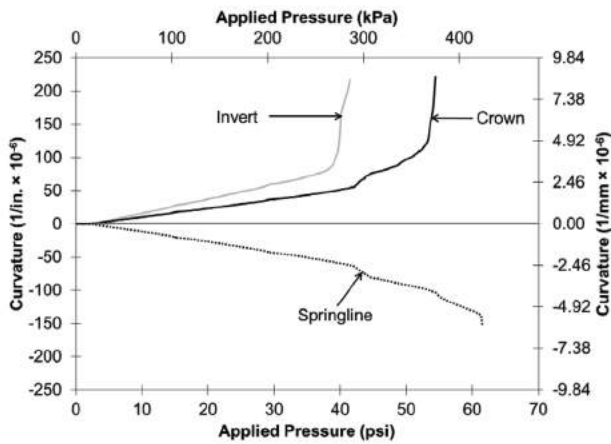
Crack widths monitored during the test of the 0.6 m (24 in.) diameter pipe under simulated deep burial are presented in Fig. 11(c). The first sign of visible cracking occurred at the invert at approximately 248 kPa (36 psi) of overburden pressure and was followed by cracking at the crown at approximately 352 kPa (51 psi) of overburden pressure. This difference was due to the development of higher moments at the invert under deep burial. The pipe reached the 0.25 mm (0.01 in.) cracking limit at an overburden pressure of approximately 414 kPa (60 psi), equivalent to 20 m (66 ft) of overburden soil.

Crack width: Program C

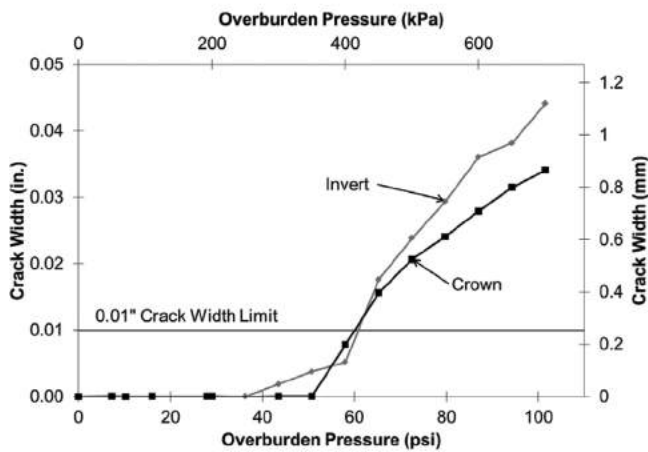
Crack widths measured during the D-load tests on the 1.2 m (48 in.) diameter pipes are presented in Fig. 10(c). The first sign of visible cracking in the Wall C pipe occurred at the invert and crown at the same load of approximately 151 kN (34 kip). The first sign of visible cracking in the



(a) Diameter change versus applied surface pressure



(b) Curvature versus applied surface pressure



(c) Crack width versus applied surface pressure.

Fig. 11—Simulated deep burial test (Program B). (Note: 1 in. = 25.4 mm.)

Wall B pipe occurred at the invert at a load of approximately 200 kN (45 kip) followed by the crown at a load of 249 kN (56 kip). According to ASTM C76-11, a Class III pipe can support a D-Load up to 65 N/m/mm (1350 lbf/ft/ft) for a maximum crack width of 0.25 mm (0.01 in.). The Wall B pipe used in the test reached the cracking limit of 0.25 mm (0.01 in.) at a D-Load of 89 N/m/mm (1862 lbf/ft/ft),

and the Wall C pipe reached the cracking limit at a D-Load of 76 N/m/mm (1581 lbf/ft/ft). This means that both pipes exceeded the load requirements of a Class III pipe, which indicates that some of the conservatism observed in the buried pipe tests is due to the pipe specimens exceeding the required capacity rather than solely being due to conservatism in the Indirect Design Method. The next section will evaluate the Indirect Design Method.

COMPARISON OF PREDICTIONS AND EXPERIMENTAL RESULTS

The results of the three-edge bearing tests conducted in Program C and from other testing as discussed previously are given in Table 3 in the column labeled “D-load”. As noted previously, the D-load and the buried pipe performance are related by bedding factors as given in Eq. (3).

$$D = \frac{W_E + W_F}{B_{FE}} + \frac{W_L}{B_{FLL}} \quad (3)$$

To determine the level of conservatism in the Indirect Design Method, an experimental live load bedding factor B_{FLL} can be calculated by rearranging Eq. (3) for B_{FLL} as all the other values in the equation, including the D-load, the live load, and the earth load that cause the critical crack to form, are known and are given in Table 3. The experimental live load bedding factor can then be compared to the live load bedding factors given by AASHTO (2012) (2.2 for 0.6 m [24 in.] pipes or 1.5 for 1.2 m [48 in.] pipes) and AASHTO (2013) (3.2 for 0.6 m [24 in.] pipes or 2.2 for 1.2 m [48 in.] pipes) to estimate the level of conservatism in the Indirect Design Method. These comparisons are given in the last two columns of Table 3. It can be seen that, although there is some conservatism in the results, the 2013 AASHTO live load bedding factors are in reasonable agreement with the experimentally determined bedding factors with a minimum difference of just 17%.

It is interesting to note that between the 2012 and 2013 AASHTO codes, the live load bedding factors for 0.3 m (1 ft) of cover changed by approximately 45%. Prior to 2013, the Indirect Design Method would have been overly conservative especially when one considers that this method is based on a serviceability limit state. In all the experiments performed herein, the bearing capacity of the ground governed the failure of the pipe system rather than the capacity of the pipe, suggesting that the governing ultimate limit state load is much higher. A similar calculation can be performed for the deep burial specimen using Eq. (3) but ignoring the live load term to determine the experimental earth load bedding factor. Based on an applied surface pressure of 414 kPa (60 psi) at cracking, the equivalent burial depth is 20.3 m (66.6 ft), resulting in a W_E of 457 kN/m (31.3 kip/ft). The experimental earth load bedding factor is 5.3 while the AASHTO earth load bedding factor is 3, resulting in a ratio of experimental to code bedding factors of 1.77. This suggests that the bedding factors for earth load may be more conservative than the live load bedding factors.

Table 3—Comparison of experimental to code-specified live load bedding factors

Specimen	W_E , kN/m (kip/ft)	Load-crack, kN (kip)	W_L , kN/m (kip/ft)	D-load, kN/m (kip/ft)	Exp. B_{FLL}	Exp./AASHTO 2012 B_{FLL}	Exp./AASHTO 2013 B_{FLL}
0.6 m (24 in.) Class IV	6.76 (0.463)	449 (101)	346 (30.8)	86 (5.89)	5.36	2.44	1.68
0.6 m (24 in.) Class V	6.76 (0.463)	325 (73.1)	250 (22.3)	89 (6.10)	3.75	1.70	1.17
1.2 m (48 in.) Wall B	12.44 (0.852)	271 (60.9)	209 (18.6)	109 (7.50)	2.58	1.72	1.17
1.2 m (48 in.) Wall C	12.76 (0.874)	334 (75.1)	257 (22.9)	91 (6.26)	3.84	2.56	1.75

CONCLUSIONS

Two 0.6 m (24 in.) diameter pipes with two different levels of reinforcement and two 1.2 m (48 in.) diameter pipes with two different wall thicknesses were tested at three different burial depths under surface loading. Additionally, a 0.6 m (24 in.) pipe was tested under simulated deep burial. In both cases, diameter change and strain was measured to develop an understanding of the performance of the pipes under the applied loads. Lastly, 1.2 m (48 in.) diameter pipes were tested in three-edge bearing to enable an evaluation of the Indirect Design Method.

Under shallow burial and service live loading, no visible cracks developed at any locations in the four specimens. At 0.3 m (1 ft) of cover and under single wheel pad loading, the 0.6 m (24 in.) Class IV and Class V-equivalent pipes developed the service limit crack width of 0.25 mm (0.01 in.) at 4.0 and 3.0 times the design service load, respectively, and the 1.2 m (48 in.) Wall B and C pipes developed the critical crack at 2.5 and 3.0 times the design service load, respectively. Under simulated deep burial, the 0.6 m (24 in.) pipe developed the service limit crack at a pressure of 414 kPa (60 psi), equivalent to a burial depth of 20 m (66 ft) in backfill of density 20.42 kN/m³ (130 lb/ft³).

The two 0.6 m (24 in.) concrete pipes were designed as Class IV and Class V-equivalent pipes, which should resist a D-load of 100N/m/mm (2000 lbf/ft/ft) and 140 N/m/mm (3000 lbf/ft/ft), respectively. From the manufacturer and previous laboratory testing it was found that the D-loads of the two 0.6 m (24 in.) test pipes were 144 and 149 N/m/mm (3008 and 3112 lbf/ft/ft) for the Class IV and V-equivalent pipes, respectively. When compared to the shallow burial tests of the same pipe, it was found that the Class IV and Class V-equivalent pipes had bedding factors 1.68 and 1.17 times the design bedding factor according to AASHTO (2013). The two 1.2 m (48 in.) pipes were designed as Class III-equivalent pipes having a cracking D-load of up to 65 N/m/mm (1350 lbf/ft/ft). The pipes tested achieved D-loads of 89 and 76 N/m/mm (1859 and 1587 lbf/ft/ft) for the Wall B and Wall C pipe, respectively. When compared to the shallow buried tests of the same pipe, it was found that the Wall B and Wall C pipe had a bedding factor 1.17 and 1.75 times the design live load bedding factor according to AASHTO (2013). This represents a significant improvement in accuracy when compared to the live load bedding factors proposed by the previous AASHTO (2012) code. For the deep burial test, the experimental earth load bedding factor to design bedding factor ratio was 1.77, suggesting that the Indirect Design Method may be more conservative in its approach to earth loads.

AUTHOR BIOS

Katrina MacDougall is an Engineer-in-Training with GHD Canada. She received her BS and MASc from Queen's University, Kingston, ON, Canada. Her research interests include the behavior of new and deteriorated reinforced concrete pipes, and design approaches for reinforced concrete pipes.

ACI member **Neil A. Hoult** is an Associate Professor in the Department of Civil Engineering at Queen's University. He received his BSc and MASc from the University of Toronto, Toronto, ON, Canada, and his PhD from the University of Cambridge, Cambridge, UK. His research interests include the behavior of reinforced concrete structures, monitoring technologies for the assessment of infrastructure, and buried structures.

Ian D. Moore is the Canada Research Chair in Infrastructure Engineering and Executive Director of GeoEngineering Centre at Queen's – RMC, at Queen's University. He received his BE and PhD from the University of Sydney, Sydney, Australia. His research interests include the development of design methods for joints in concrete culverts, strength of deteriorated steel and reinforced concrete culverts, and performance and design of liners used to repair sewers and culverts.

ACKNOWLEDGMENTS

The authors would like to acknowledge the contribution of a number of individuals to the paper, including G. Boyd, the geotechnical lab technician, B. Westervelt, and T. Smith, who provided valuable assistance during the testing process, as well as provision of the test pipes by Hanson and M-Con as arranged by P. Imm of the Ontario Concrete Pipe Association. This research was funded by the National Cooperative Highway Research Program (NCHRP) through the Transportation Research Board of the National Academy of Sciences, Washington, DC. The findings, conclusions, or recommendations expressed in this paper do not necessarily reflect the views of the sponsors.

NOTATION

B_c	=	outer diameter of the pipe, in m (ft)
B_{FE}	=	earth load bedding factor = 3 for 0.6 m (24 in.) pipes or 2.87 for 1.2 m (48 in.) pipes
B_{FLL}	=	live load bedding factor
D	=	D-load of pipe, in kN/m (kip/ft)
F_E	=	vertical arching factor = 1.4 for Type 2 installation
H	=	height of soil above crown, m (ft)
h	=	pipe wall thickness, mm (in.)
W_E	=	unfactored earth load, kN/m (kip/ft) = $F_E w B_c H$
W_F	=	unit weight of fluid in pipe, taken as 0 for the tests
W_L	=	unfactored live load, kN/m (kip/ft) = surface load/(wheel pad width + 1.15 × H)
w	=	unit weight of soil assumed to be 20.42 kN/m ³ (0.130 kip/ft ³)
$\epsilon_{average}$	=	average circumferential strain
ϵ_{inside}	=	circumferential strain measured on inside face of pipe
$\epsilon_{outside}$	=	circumferential strain measured on outside face of pipe
ϕ	=	change in curvature in 1/mm (1/in.)

REFERENCES

- AASHTO, 2012, "AASHTO LRFD Bridge Design Specifications," sixth edition, American Association of Highway and Transportation Officials, Washington, DC, 1661 pp.
- AASHTO, 2013, "AASHTO LRFD Bridge Design Specifications, sixth edition, 2013 Interim Revisions," American Association of Highway and Transportation Officials, Washington, DC, 1925 pp.
- ASTM C76-11, 2011, "Standard Specification for Reinforced Concrete Culvert, Storm Drain, and Sewer Pipe," ASTM International, West Conshohocken, PA, 11 pp.

- ASTM C497-13, 2013, "Standard Test Methods for Concrete Pipe, Manhole Sections or Tile," ASTM International, West Conshohocken, PA, 14 pp.
- ASTM C655M-14, 2014, "Standard Specification for Reinforced Concrete D-Load Culvert, Storm Drain, and Sewer Pipe (metric)," ASTM International, West Conshohocken, PA, 6 pp.
- Becerril García, D., 2012, "Investigation of Culvert Joints Employing Large Scale Tests and Numerical Simulations," PhD thesis, Department of Civil Engineering, Queen's University at Kingston, Kingston, ON, Canada, 397 pp.
- Becerril García, D., and Moore, I. D., 2013, "Response of Bell and Spigot Joints in Culverts under Vehicle Load," The 4th International Conference on Pipelines and Trenchless Technology, Xian, China, pp. 1140-1150.
- CSA, 2006, "Canadian Highway Bridge Design Code (CAN/CSA-S06-06)," Canadian Standards Association, Mississauga, ON, Canada, 930 pp.
- Destrebecq, J. F.; Toussaint, E.; and Ferrier, E., 2011, "Analysis of Cracks and Deformations in a Full Scale Reinforced Concrete Beam Using a Digital Image Correlation Technique," *Experimental Mechanics*, V. 51, No. 6, pp. 879-890. doi: 10.1007/s11340-010-9384-9
- Dutton, M.; Take, W. A.; and Hoult, N. A., 2014, "Curvature Monitoring of Beams Using Digital Image Correlation," *Journal of Bridge Engineering*, ASCE, V. 19, No. 3, p. 05013001 doi: 10.1061/(ASCE)BE.1943-5592.0000538
- Erdogmus, E., and Tadros, M., 2009, "Behavior and Design of Buried Concrete Pipe—Phase 2," Nebraska Department of Roads, Lincoln, NE, 124 pp.
- Hoult, N. A.; Take, W. A.; Lee, C.; and Dutton, M., 2013, "Experimental Accuracy of Two Dimensional Strain Measurements Using Digital Image Correlation," *Engineering Structures*, V. 46, pp. 718-726. doi: 10.1016/j.engstruct.2012.08.018
- Küntz, M.; Jolin, M.; Bastien, J.; Perez, F.; and Hild, F., 2006, "Digital Image Correlation Analysis of Crack Behavior in a Reinforced Concrete Beam During a Load Test," *Canadian Journal of Civil Engineering*, V. 33, No. 11, pp. 1418-1425. doi: 10.1139/106-106
- Lay, G. R., and Brachman, R. W. I., 2014, "Full-Scale Physical Testing of a Buried Reinforced Concrete Pipe under Axle Load," *Canadian Geotechnical Journal*, V. 51, No. 4, pp. 394-408. doi: 10.1139/cgj-2012-0256
- McGrath, T. J., 1993, "Design of Reinforced Concrete Pipe: A Review of Traditional and Current Methods," The Second Conference on Structural Performance of Pipes, Columbus, OH, pp. 14-17.
- Moore, I. D., 2012, "Large-Scale Laboratory Experiments to Advance the Design and Performance of Buried Pipe Infrastructure," 2nd International Conference on Pipelines and Trenchless Technology, Wuhan, China, 11 pp.
- Moore, I. D.; Becerril Garcia, D.; Sezen, H.; and Sheldon, T., 2012, "NCHRP Web-Only Document 190: Structural Design Requirements for Culvert Joints," Transportation Research Board, Washington DC, 387 pp.
- Take, W. A., 2015, "Thirty-Sixth Canadian Geotechnical Colloquium: Advances in Visualization of Geotechnical Processes through Digital Image Correlation," *Canadian Geotechnical Journal*, doi: 10.1139/cgj-2014-0080.10.1139/cgj-2014-0080
- Tognon, A. R.; Rowe, R. K.; and Brachman, R. W. I., 1999, "Evaluation of Side Wall Friction for a Buried Pipe Testing Facility," *Geotextiles and Geomembranes*, V. 17, No. 4, pp. 193-212. doi: 10.1016/S0266-1144(99)00004-7
- White, D. J.; Take, W. A.; and Bolton, M. D., 2003, "Soil Deformation Measurement Using Particle Image Velocimetry (PIV) and Photogrammetry," *Geotechnique*, V. 53, No. 7, pp. 619-631. doi: 10.1680/geot.2003.53.7.619
- Wong, L. S.; Allouche, E. N.; Dhar, A. S.; Baumert, M.; and Moore, I. D., 2006, "Long Term Monitoring of SIDD Type IV Installations," *Canadian Geotechnical Journal*, V. 43, No. 4, pp. 392-408. doi: 10.1139/t06-012

NOTES:
